

## Accepted Manuscript

A mimetic of the mSin3-binding helix of NRSF/REST ameliorates abnormal pain behavior in chronic pain models

Hiroshi Ueda, Jun-ichi Kurita, Hiroyuki Neyama, Yuuka Hirao, Hiroyuki Kouji, Tadashi Mishina, Masaji Kasai, Hirofumi Nakano, Atsushi Yoshimori, Yoshifumi Nishimura

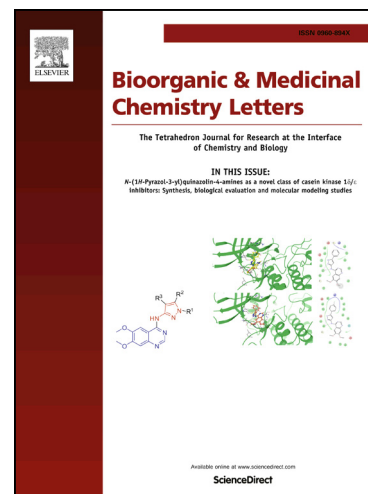
PII: S0960-894X(17)30887-9  
DOI: <http://dx.doi.org/10.1016/j.bmcl.2017.09.006>  
Reference: BMCL 25270

To appear in: *Bioorganic & Medicinal Chemistry Letters*

Received Date: 8 August 2017  
Revised Date: 1 September 2017  
Accepted Date: 1 September 2017

Please cite this article as: Ueda, H., Kurita, J-i., Neyama, H., Hirao, Y., Kouji, H., Mishina, T., Kasai, M., Nakano, H., Yoshimori, A., Nishimura, Y., A mimetic of the mSin3-binding helix of NRSF/REST ameliorates abnormal pain behavior in chronic pain models, *Bioorganic & Medicinal Chemistry Letters* (2017), doi: <http://dx.doi.org/10.1016/j.bmcl.2017.09.006>

This is a PDF file of an unedited manuscript that has been accepted for publication. As a service to our customers we are providing this early version of the manuscript. The manuscript will undergo copyediting, typesetting, and review of the resulting proof before it is published in its final form. Please note that during the production process errors may be discovered which could affect the content, and all legal disclaimers that apply to the journal pertain.



**A mimetic of the mSin3-binding helix of NRSF/REST ameliorates abnormal pain behavior in chronic pain models**

Hiroshi Ueda <sup>a</sup>, Jun-ichi Kurita <sup>b</sup>, Hiroyuki Neyama <sup>a</sup>, Yuuka Hirao <sup>b</sup>, Hiroyuki Kouji <sup>c,d</sup>, Tadashi Mishina <sup>c</sup>, Masaji Kasai <sup>c</sup>, Hirofumi Nakano <sup>c,e</sup>, Atsushi Yoshimori <sup>f</sup>, and Yoshifumi Nishimura <sup>b,\*</sup>

<sup>a</sup> Department of Pharmacology and Therapeutic Innovation, Nagasaki University Graduate School of Biomedical Sciences, Nagasaki 852-8521, Japan

<sup>b</sup> Graduate School of Medical Life Science, Yokohama City University, 1-7-29 Suehiro-cho, Tsurumi-ku, Yokohama 230-0045, Japan

<sup>c</sup> PRISM BioLab Co., Ltd., 4259-3, Nagatsuda-cho, Midori-ku, Yokohama 226-8510, Japan

<sup>d</sup> Oita University, Faculty of Medicine, 1-1, Idaigaoka, Hasama-machi, Yufu-city, Oita, 879-5593, Japan

<sup>e</sup> Kitasato University, Kitasato Life Science Institute, 5-9-1 Shirokane, Minato-ku, Tokyo 108-8641, Japan

<sup>f</sup> Institute of Theoretical Medicine, Inc., , 4259-3, Nagatsuda-cho, Midori-ku, Yokohama 226-8510, Japan

\*Corresponding author at: Graduate School of Medical Life Science, Yokohama City

University, 1-7-29 Suehiro-cho, tsurumi-ku, Yokohama 230-0045, Japan

*E-mail address:* [nisimura@yokohama-cu.ac.jp](mailto:nisimura@yokohama-cu.ac.jp)

**Key Words:** NRSF/REST, mSin3, NMR, fibromyalgia, neuropathic pain

### ***Abbreviations***

MOPr,  $\mu$ -opioid receptor; NRSF, neuron-restrictive silencer factor; REST, repressor element 1 silencing transcription factor; HDAC, histone deacetylase; nrse, neural restrictive silencer element; re1, repressor element 1; PAH, paired amphipathic helix; STD, saturation transfer difference; HSQC, heteronuclear single quantum coherence; CSP, chemical shift perturbation; ICS, intermittent cold stress; IPS, intermittent psychological stress; PWL, paw withdrawal latency; pSNL, partial sciatic nerve ligation

**ABSTRACT**

**The neuron-restrictive silencing factor NRSF/REST binds to neuron-restrictive silencing elements in neuronal genes and recruits corepressors such as mSin3 to inhibit epigenetically neuronal gene expression. Because dysregulation of NRSF/REST is related to neuropathic pain, here, we have designed compounds to target neuropathic pain based on the mSin3-binding helix structure of NRSF/REST and examined their ability to bind to mSin3 by NMR. One compound, mS-11, binds strongly to mSin3 with a binding mode similar to that of NRSF/REST. In a mouse model of neuropathic pain, mS-11 was found to ameliorate abnormal pain behavior and to reverse lost peripheral morphine analgesia. Furthermore, even in the less well epigenetically defined case of fibromyalgia, mS-11 ameliorated symptoms in a mouse model, suggesting that fibromyalgia is related to the dysfunction of NRSF/REST. Taken together, these findings show that the chemically optimized mimetic mS-11 can inhibit mSin3-NRSF/REST binding and successfully reverse lost peripheral morphine analgesia in mouse models of pain.**

Epigenetics is a challenging but promising topic for better understanding of genetic memory, and much literature has been published on the epigenetic regulation of chronic pain,<sup>1</sup> which involves an aspect of pain memory. The design of chemicals to affect the genetic/epigenetic regulation of key molecules involved in pain processing is therefore expected to provide a new medicinal solution for intractable chronic pain.<sup>2,3</sup>

Nerve injury-induced neuropathic pain is characterized by negative signs such as unique hyposensitivity to C-fiber pain fiber stimulation and loss of peripheral morphine analgesia, as well as conventional positive signs including hyperalgesia and allodynia.<sup>4</sup> Recent studies have revealed that the negative factors are attributed to epigenetic silencing of the C-fiber Na<sub>v</sub>1.8 channel and  $\mu$ -opioid receptor (MOPr) through mechanisms involving a repressor, neuron-restrictive silencing factor (NRSF; also known as repressor element 1 silencing transcription factor, REST),<sup>5</sup> together with histone deacetylase (HDAC).<sup>6,7</sup>

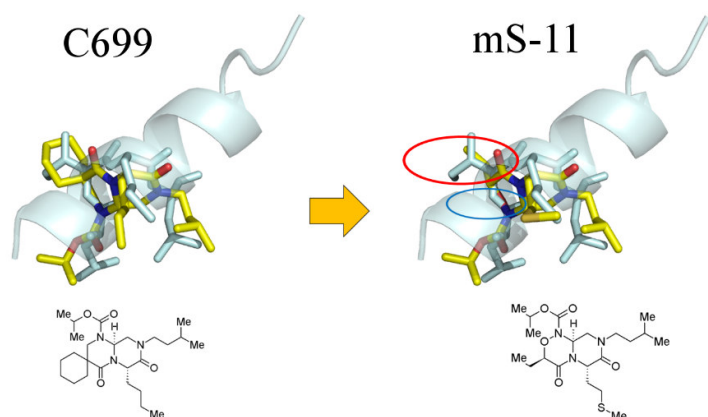
NRSF/REST was originally identified as an essential transcriptional repressor that inhibits the expression of neuronal genes in both non-neuronal cells and neuronal progenitor cells. It binds to a 21-base-pair DNA element, termed neuron restrictive silencer element (nrse) or repressor element 1 (re1), of which approximately 1900 copies are found in the human genome.<sup>8</sup> The N-terminal repressor domain of NRSF/REST recruits a corepressor, mSin3,<sup>4</sup> which consists of four paired amphipathic helix (PAH) domains, termed PAH1-PAH4. The structure of the PAH1 domain of mSin3B, an isoform of mSin3, in complex with the N-terminal repressor domain of NRSF/REST was previously determined by NMR: the minimal repressor domain of NRSF/REST is an intrinsically disordered domain containing 44-54 N-terminal amino acid residues that form an  $\alpha$  helix after binding to the mSin3B PAH1 domain

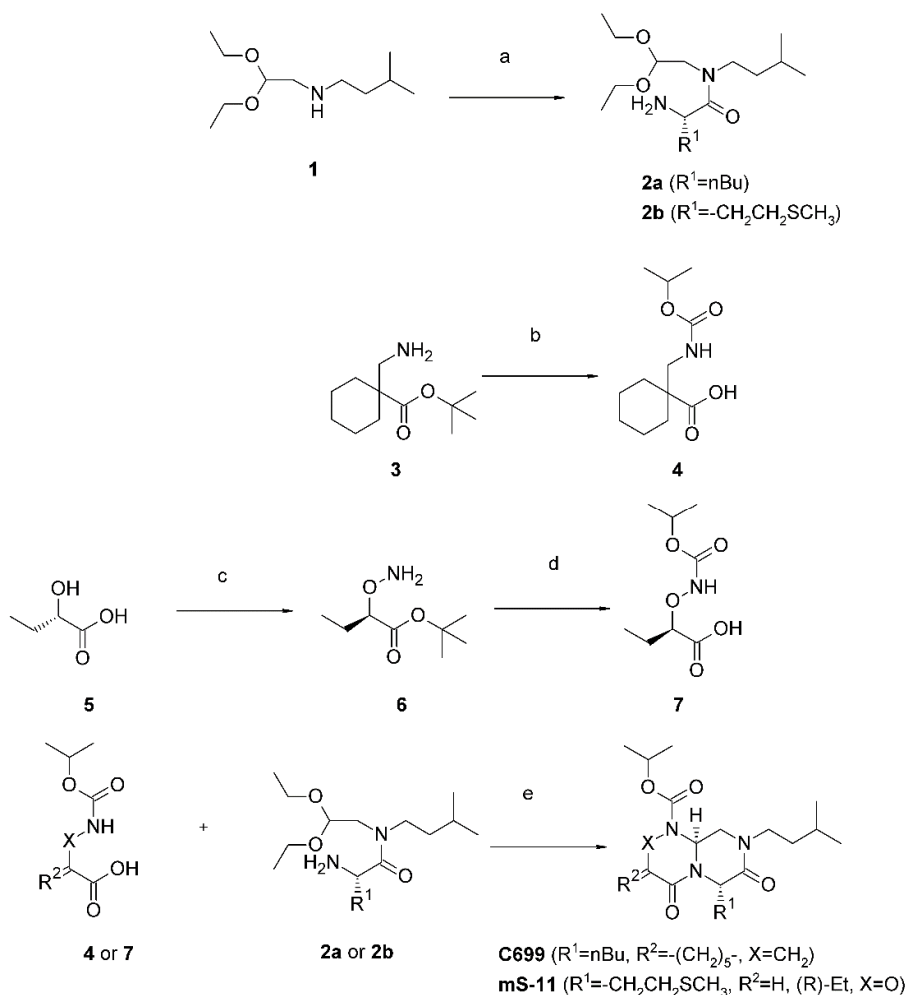
(Supplementary figure S1).<sup>9</sup> In the complex structure, four hydrophobic amino acids of NRSF/REST — namely, leucine at position 46 (Leu46), isoleucine at 47 (Ile47), methionine at 48 (Met48) and leucine at 49 (Leu49) — interact deeply with the hydrophobic groove of the mSin3B PAH1 domain. We therefore considered that a compound mimicking the one helix turn formed by these four amino acids of NRSF/REST might bind to the mSin3 PAH1 domain and inhibit the function of NRSF/REST.

Recently, investigators are also becoming interested in a molecular understanding of the poorly investigated disorder fibromyalgia, a predominantly female syndrome of generalized pain,<sup>10,11</sup> and several experimental pain models mimicking clinical features of its pathophysiology and pharmacotherapy have been developed.<sup>12,13</sup> Both in these pain models and in patients, a lack of central morphine analgesia has been observed, suggesting that negative regulatory mechanisms may derive epigenetic silencing in fibromyalgia, as in the case of neuropathic pain. To improve understanding of the molecular mechanisms underlying the unique phenomena in fibromyalgia, we aimed to investigate the effect of mimetic inhibitors of NRSF/REST in fibromyalgia models as well as in neuropathic pain models.

PRISM BioLab has developed many helix mimetic templates (>30) for drug discovery purposes. We analyzed these templates by superimposing them on the one helix turn of NRSF/REST described above (Leu46, Ile47, Met48, and Leu49; hereafter termed the “target helix”). Ultimately, one of the templates that mimicked the main chain conformations of the target helix was selected. By adding the amino acid side chain structures of the target helix loop to the template, C699 (Fig. 1) was

designed and synthesized by the synthetic route shown in Scheme 1.<sup>14</sup>



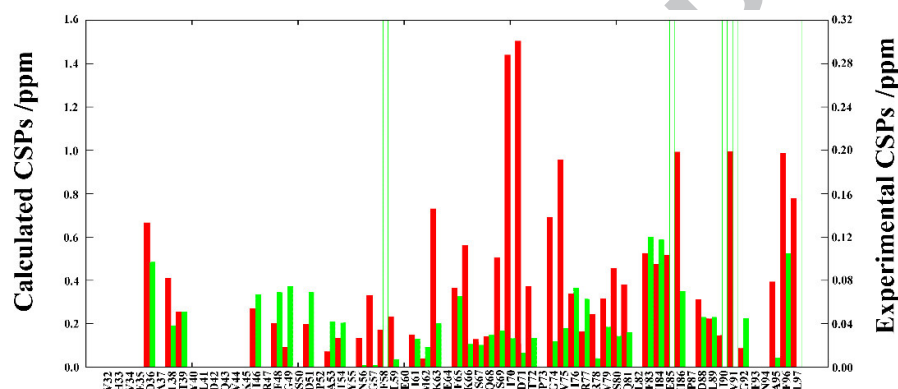


Next, to improve the solubility and structural similarity of C699 to the target helix, we synthesized mS-11 (Fig. 1) in accordance with Scheme 1.<sup>14</sup> The two main modifications of mS-11 from C699 were as follows: first, displacement of the isoleucine position from spiro-cyclohexyl to (*R*)-ethyl was performed to achieve as structure closer to the natural isoleucine side chain; second, pyrimidine was converted to an oxadiazine ring to improve the solubility of C699. The chemical structures of C699 and mS-11 were confirmed by NMR and other analytical methods (Supplementary Information).



The ability of both C699 and mS-11 to bind to the mSin3B PAH1 domain was examined by NMR using saturation transfer difference (STD)<sup>15,16</sup>, Waterlogsy<sup>17-19</sup> and <sup>1</sup>H-<sup>15</sup>N heteronuclear single quantum coherence (HSQC)<sup>20</sup> titration experiments, which showed that mS-11 bound more strongly to the mSin3B PAH1 domain than C699 (Supplementary Fig. S2).

In the HSQC experiments (Supplementary Fig. S3 and S4), chemical shift changes were compared between unbound mSin3B PAH1 and bound mSin3B PAH1 under the condition of a 10-fold excess of mS-11 (Fig. 2, green lines).

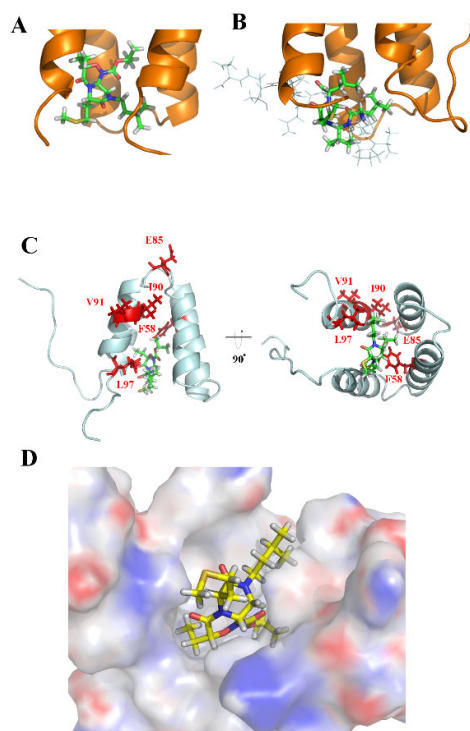


The CSPs for mS-11 were delocalized over almost all of the molecular surface of the mSin3B PAH1 domain; thus, it was hard to identify the contact site of the PAH1 domain for mS-11 from only the experimental CSPs. After binding to mS-11, the structure of the mSin3B PAH1 domain is likely to change, as observed when it binds to NRSF/REST, and to lead to changes in its CSPs. It was therefore necessary to differentiate the CSPs due solely to structural change effects after mS-11 binding from those due solely to contact effects with mS-11.

First, we estimated the CSPs due solely to structural changes of mSin3B PAH1 caused by binding to NRSF/REST by applying SHIFTX2<sup>21</sup> calculations to two mSin3B PAH1 domain structures: a ligand-free form (PDB code: 2CR7), and an

NRSF/REST-bound form (PDB code: 2CZY), as shown in Fig. 2 (red). The CSPs calculated to be due to only structural changes after binding to NRSF/REST were larger than the experimental CSPs observed for binding to mS-11 (Fig. 2, right and left side axes). This suggests that the structure of the mSin3B PAH1 domain bound to mS-11 is more similar to the unbound structure than to the NRSF/REST bound structure; thus, the binding affinity between mS-11 and PAH1 is not as strong as that between NRSF/REST and PAH1. Although the CSPs caused by mS-11 are small, the pattern of CSPs for mS-11 is very close to that of CSPs calculated to be due solely to structural changes induced by NRSF/REST binding (Fig. 2), suggesting that the binding mode of mS-11 is similar to that of NRSF/REST. In addition, the HSQC signals of five residues of the mSin3 PAH1 domain (Phe58, Glu85, Ile90, Val91 and Leu97) are disappeared (Fig. 2, green blank bars); these amino acids are likely to contact mS-11 under fluctuating conditions. In particular, the CSP of Phe58 was calculated as a small CSP due only to structural changes in mSin3 PAH1 after binding to NRSF/REST; however, disappearance of the Phe58 signal suggested that Phe58 is a key residue for contact with PAH1. For the subsequent docking calculation, therefore, we defined the residues that disappeared due to ligand contact as active residues, and the neighboring residues as passive residues.

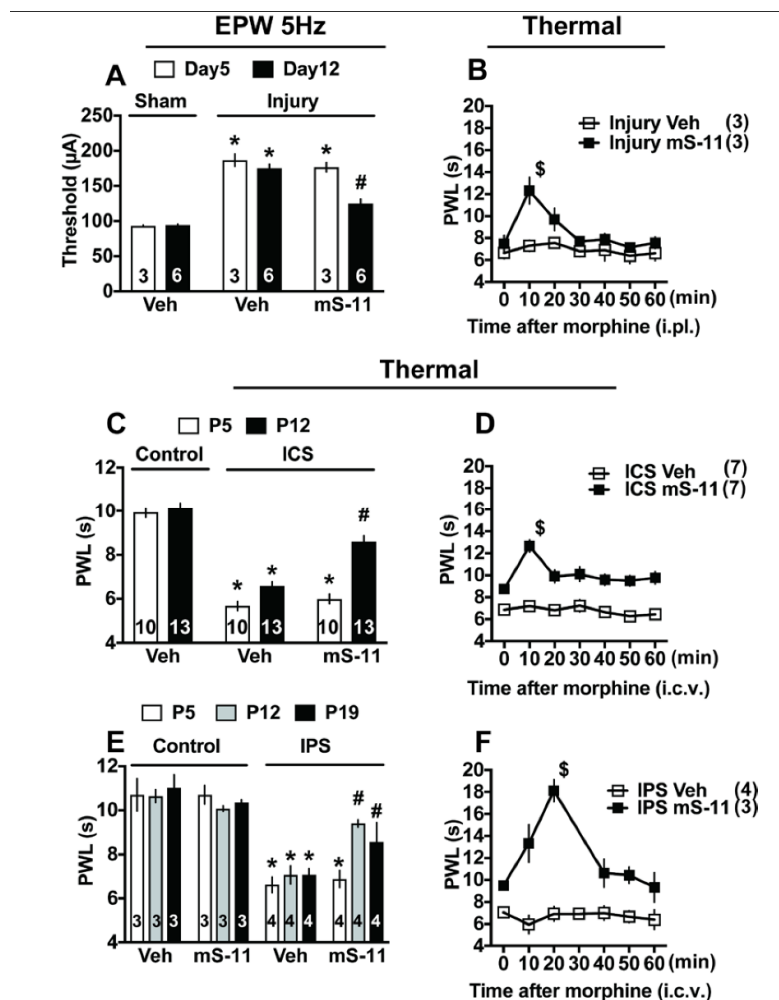
Figure 3A shows the structure of mS-11 docked onto the mSin3B PAH1 domain using HADDOCK (PDB code; 5Y95).



Notably, mS-11 inserts more deeply into the mSin3B PAH1 domain as compared with the NRSF peptide (Fig. 3B). In detail, two of the active five residues, Phe58 and Leu97, make direct contacts with mS-11, while the other three residues, Glu85, Ile90 and Leu97, are not directly involved in the interaction (Fig. 3C). We considered that the disappearance of the signals of these three residues must be caused by a characteristic structural change of the PAH1 domain on binding. The docking structure also supports the higher affinity of mS-11 binding to mSin3B relative to C699 binding: the ethyl-group of mS-11, which corresponds to the spiro-cyclohexyl group of C699, inserts more deeply to the hydrophobic pocket (Fig. 3D).

We tested the effects of mS-11 in a mouse model of neuropathic pain. The nociceptive threshold to C-fiber stimulation (5 Hz) was significantly increased in mice on day 5 after partial sciatic nerve ligation (pSNL) injury, as shown in Fig. 4A. As

predicted, this hyposensitivity (hypoesthesia) was significantly reversed on day 12 after daily treatment with 10 mg/kg (i.p.) of mS-11 from day 5 to day 11.



In addition, morphine analgesia lost in the pSNL model was recovered, as predicted (Fig. 4B).

We further investigated the recovery of lost morphine analgesia in a mouse model of fibromyalgia. Intermittent cold stress (ICS)-treated mice were given mS-11 as described above for the pSNL model. Repeated mS-11 treatment reversed both the hyperalgesia and the loss of morphine analgesia (Fig. 4C,D). Similar recovery of hyperalgesia and loss of morphine analgesia were observed on repeated mS-11 treatments in a recently

developed fibromyalgia-like pain mode induced by intermittent physiological stress (IPS), as shown in Fig. 4E,F.

The present study has provided experimental evidence showing that mS-11, a compound chemically optimized to interact with mSin3 and to inhibit mSin3-NRSF/REST binding, successfully reversed the lost peripheral morphine analgesia which caused by epigenetic MOPr gene silencing through NRSF and HDAC molecules<sup>4</sup> in a model of neuropathic pain. Therefore, these findings suggest that mSin3 may play an important role in this silencing machinery. The successful reversal of pain symptoms was also observed in the case of loss of central morphine analgesia in two models of stress-induced fibromyalgia (ICS and IPS), although the time-consuming identification of the brain loci involved remains a subject for future study.

Interestingly, we observed that hyperalgesia in both the ICS and IPS models was reversed by repeated mS-11 treatment, in contrast to the finding that C-fiber hyposensitivity is reversed in the model of neuropathic pain. Because abnormal pain behavior in the ICS or IPS model is closely related to centrally originating pain mechanisms<sup>13</sup>, whereas the neuropathic pain model is based on peripheral mechanisms causing A $\beta$ /A $\delta$ -fiber hyperalgesia and C-fiber hypoesthesia, it remains unclear whether similar machineries are involved in the central and peripheral actions of mS-11. It is interesting to speculate that the paradoxical anti-hyperalgesic action of mS-11 may arise because it prevents the decrease in the endogenous opioid analgesic system<sup>13</sup> by blocking in the epigenetic silencing of MOPr gene expression.

### Acknowledgements

This work was supported in part by Grants-in-Aid for an NMR platform [07022019]

(Y.N.) from the Ministry of Education, Culture, Sports, Science and Technology (MEXT), Japan; the Platform for Drug Discovery, Informatics, and Structural Life Science [16am0101033j0004] (Y.N.) and [16am0101012j0005] (H.U.) from the Japan Agency for Medical Research and Development (AMED), Japan; and JSPS KAKENHI Grant Numbers JP17H01586 (H.U.) and JP26253077 (H.U.). This paper is also based on results obtained from the Innovation Commercialization Venture Support Project, subsidized by the New Energy and Industrial Technology Development Organization (NEDO).

#### **A. Supplementary data**

Supplementary data associated with this article can be found in the online version at .

#### **References and Note**

1. Descalzi, G.; Ikegami, D.; Ushijima, T.; Nestler, E.; Zachariou, V.; Narita, M. *Trends in Neuroscience* **2015**, 38, 237-46.

2. Stranowska, J.; Costante, R.; Guillemyn, K.; Popiolek-Barczyk, K.; Chung, N.-N.; Lemieux, C.; Keresztes, A.; Duppen, J.-V.; Mollica, A.; Strecher, J.; Broeck, J.-V.; Schiller, P.-W.; Tourwe, D.; Mika, J.; Ballet, S.; Przewlocka, B. *ACS Chem. Neurosci.* **2017**, DOI:10.102/acschemneuro. 7b00226.
3. Stefanucci, A.; Mosquera, J.; Vazuquz, E.; Mascarenas, J.-L.; Novellio, E.; Mollica, A. *ACS Med. Chem. Lett.* **2015**, *6*, 1220-4.
4. Matsumoto, M.; Inoue, M.; Hald, A.; Yamaguchi, A.; Ueda, H. *Mol. Pain* **2006**, *2*, 16.
5. Chong, J. A.; Tapia-Ramírez, J.; Kim, S.; Toledo-Aral, J. J.; Zheng, Y.; Boutros, M. C.; Altshuller, Y. M.; Frohman, M. A.; Kraner, S. D.; Mandel, G. *Cell* **1995**, *80*, 949–57.
6. Naruse, Y.; Aoki, T.; Kojima, T.; Mori, N. *Proc. Natl. Acad. Sci. U. S. A.* **1999**, *96*, 13691–6.
7. Uchida, H.; Ma, L.; Ueda, H. *J. Neurosci.* **2010**, *30*, 4806–14.
8. Bruce, A. W.; Donaldson, I. J.; Wood, I. C.; Yerbury, S. A.; Sadowski, M. I.; Chapman, M.; Göttgens, B.; Buckley, N. J. *Proc. Natl. Acad. Sci. U. S. A.* **2004**, *101*, 10458–63.
9. Nomura, M.; Uda-Tochio, H.; Murai, K.; Mori, N.; Nishimura, Y. *J. Mol. Biol.* **2005**, *354*, 903–15.
10. Theoharides, T. C.; Tsilioni, I.; Arbetman, L.; Panagiotidou, S.; Stewart, J. M.; Gleason, R. M.; Russell, I. J. *J. Pharmacol. Exp. Ther.* **2015**, *355*, 255–63.
11. Sluka, K. A.; Clauw, D. J. *Neuroscience* **2016**, *338*, 114–129.
12. Nishiyori, M.; Ueda, H. *Mol. Pain* **2008**, *4*, 52.
13. Ueda, H.; Neyama, H. *Neurobiol. Pain* **2017**, *1*, 16–25.

14. The synthesis of **C699** and **mS-11** is as follows. Amine parts, **2a** and **2b**, were prepared by condensation of amine **1** and N-protected amino acids, followed by deprotection of Cbz- or Fmoc-groups. Carboxylic acid part **4** of **C699** was derived from amino acid ester **3** by reaction with isopropyl chloroformate and with formic acid. Carboxylic acid part **7** of **mS-11** was prepared from amino alcohol **5**, which was subjected to esterification, Mitsunobu reaction and deprotection to afford hydroxylamine **6**. The hydroxylamine **6** was converted to acid part **7** by the similar methods **4** to **5**. The amine part, **2a** or **2b**, was coupled with the acid parts, **4** or **7**, using condensation reagent, and was treated with formic acid to afford the desired compound, **C699** or **mS-11**, respectively.
15. Mayer, M.; Meyer, B. *J. Am. Chem. Soc.* **2001**, *123*, 6108–17.
16. Meyer, B.; Peters, T. *Angew. Chem. Int. Ed. Engl.* **2003**, *42*, 864–90.
17. Dalvit, C.; Fogliatto, G.; Stewart, A.; Veronesi, M.; Stockman, B. *J. Biomol. NMR* **2001**, *21*, 349–59.
18. Dalvit, C.; Pevarello, P.; Tatò, M.; Veronesi, M.; Vulpetti, A.; Sundström, M. *J. Biomol. NMR* **2000**, *18*, 65–8.
19. Antanasijevic, A.; Ramirez, B.; Caffrey, M. *J. Biomol. NMR* **2014**, *60*, 37–44.
20. Davis, A. L.; Keeler, J.; Laue, E. D.; Moskau, D. *J. Magn. Reson.* **1992**, *98*, 207–216.
21. Han, B.; Liu, Y.; Ginzinger, S. W.; Wishart, D. S. *J. Biomol. NMR* **2011**, *50*, 43–57.



## Figure Legends

**Figure 1.** Structural comparison of the NRSF/REST helix with C699 and mS-11.

The spiro-cyclohexyl group in C699 was changed into an ethyl group in mS-11 to improve structural similarity to the natural isoleucine; in addition, a pyrimidine ring in C699 was changed into an oxadiazine ring to improve solubility.

**Figure 2.** CSPs of the mSin3B PAH1 domain binding to mS-11.

Chemical shift changes in the mSin3B PAH1 domain after the addition of mS-11.

Shown are the experimental CSPs measured for mS-11 addition (left axis, green lines) and the CSPs calculated for PAH1 binding to the NRSF/peptide (right axis, red lines).

**Figure 3.** The structure of the mSin3B PAH1 domain bound to mS-11.

(A) Structure of the mSin3B PAH1 domain (orange ribbon) bound to mS-11 (stick model). The four interacting hydrophobic amino acids are indicated. (B) Structure of the mSin3B PAH1 domain (orange ribbon) bound to the NRSF/REST peptide (stick model). The four interacting hydrophobic amino acids are indicated. (C) Structure of the mSin3B PAH1 domain (pale cyan ribbon) bound to mS-11. The five active residues in the HADDOCK calculations are indicated by red sticks. (D) Surface structure of the mSin3B PAH domain with mS-11 docked.

**Figure 4.** Repeated treatment with mS-11 ameliorates abnormal pain behavior in mouse models of neuropathic pain and fibromyalgia.

(A, B) C-fiber hypoesthesia (A) and loss of peripheral morphine analgesia (B) on day 5

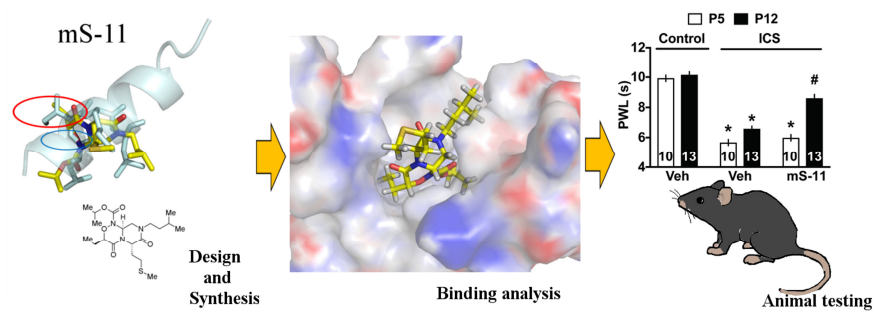
after pSNL injury, and their reversals on day 12 after treatment with 10 mg/kg i.p. of mS-11 (days 5–11). Results are represented as Threshold ( $\mu$ A, **A**), or paw withdrawal latency (PWL, s, **B**). \* $p < 0.05$ , vs. Sham-Vehicle on each corresponding day. # $p < 0.05$ , vs. Injury-mS-11 (day 5). \$ $p < 0.05$ , vs. PWL at 0 min. (**C**, **D**) Thermal hyperalgesia (**C**) and loss of central morphine analgesia (**D**) on day 5 post ICS (P5), and their reversal on P12 after daily treatment with 10 mg/kg i.p. of mS-11 (days 5–11). (**E**, **F**) Thermal hyperalgesia (**E**) and loss of central morphine analgesia (**F**) on days 5, 12, and 19 post IPS (p5, P12, and P19), and their reversal on P12 and P19 by daily treatment with 10 mg/kg i.p. of mS-11 (days 5–11). \* $P < 0.05$ , vs. PWL at P5 (IPS-mS-11). \$ $p < 0.05$ , vs. PWL at 0 min. The number of mice used in each group is indicated in figures (**A–F**).

### Scheme Legend

#### Scheme 1.

Synthesis of C699 and mS-11. The following reagents and conditions were used in each step. (a) (i) Cbz-norLeu-OH or Fmoc-Met-OH, HATU, DIEA,  $\text{CH}_2\text{Cl}_2$  (DCM); (ii)  $\text{H}_2$ , Pd-C, MeOH or piperidine, DCM. (b) (i)  $i\text{-PrOCOC}\text{Cl}$ ,  $\text{Et}_3\text{N}$ , DCM; (ii)  $\text{HCOOH}$ . (c) (i)  $\text{AcCl}$  (ii)  $t\text{-BuOH}$ , DMAP, DCC, DCM; (iii)  $\text{K}_2\text{CO}_3$ , MeOH,  $\text{H}_2\text{O}$ ; (iv)  $N\text{-hydroxyphthalimide}$ ,  $\text{Ph}_3\text{P}$ , DEAD, THF; (v) hydrazine hydrate, MeOH. (d) (i)  $i\text{-PrOCOC}\text{Cl}$ , pyridine,  $\text{CH}_3\text{CN}$ ; (ii)  $\text{HCOOH}$ . (e) (i) HATU, DIEA, DCM or DMT-MM, NMM, MeOH; (ii)  $\text{HCOOH}$ .

Graphical abstract



**Highlights**

- Dysregulation of the neural repressor, NRSF is related to neuropathic pain.
- Based on the structure of NRSF bound to mSin3, mS-11 was designed and synthesized.
- NMR shows that the mS-11 binding site on mSin3 is similar to that of NRSF.
- mS-11 reverses hyposensitivity of the peripheral C-fiber response in neuropathy.
- mS-11 reverses hypersensitivity of hyperalgesia/allodynia in a fibromyalgia model.